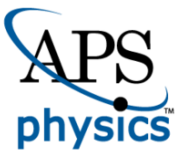

Rheology of Dense Granular Mixtures: Boundary Pressures

K. M. Hill and B. Yohannes

Phys. Rev. Lett. **106**, 058302 — Published 4 February 2011

DOI: 10.1103/PhysRevLett.106.058302

Rheology of Dense Granular Mixtures: Boundary Pressures

K. M. Hill and B. Yohannes

Saint Anthony Falls Laboratory, Department of Civil Engineering,

University of Minnesota, Minneapolis, MN 55414

Abstract

Models for dense sheared granular materials indicate that their rheological properties depend on particle size, but the representative size for mixtures is not obvious. Here, we computationally study pressure on a boundary due to sheared granular mixtures to determine its dependence on particle size distribution. We find that the pressure does not depend monotonically on average particle size. Instead it has an additional dependence on a measure of the effective free volume per particle we adapt from an expression for packing of monosized particles near the jammed state.

PACS numbers: 47.57.Gc, 47.57.Qk, 81.05.Rm, 83.10.Pp, 92.40.Ha

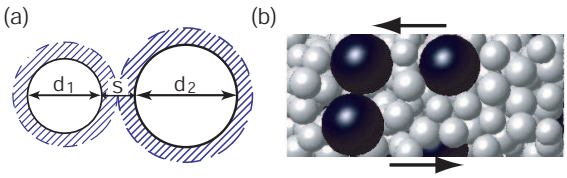

FIG. 1: (a) Sketch of s and d from Equation 2. Hatched region indicates an effective free volume described later in the text. (b) Image from a small section of the simulated sheared particles described in the text.

The ability to predict the stresses particulate mixtures exert on their boundaries is important for many critical natural and industrial applications. For example, predicting boundary stresses due to bouldery debris flows – massive flows of rocks and boulders – is important for understanding landscape morphology as well as for hazard mitigation [1]-[4]. Additionally, wear associated with boundary stresses can considerably shorten the life of industrial machinery [5]. However, a predictive model for stresses due to dense sheared granular mixtures is elusive.

A formulation proposed by Bagnold in the 1950's [6] has held for monodisperse systems in a general sense, far beyond the regime of rapid collisional flows for which it was derived, provided the particles are sufficiently hard [7]. Based on considerations of momentum transfer via collisions in sheared flows, Bagnold proposed the average pressure p scales with both the particle size d and the shear rate $\dot{\gamma}$ squared with some form of the structure ξ:

$$p \sim f(\xi)\rho d^2\dot{\gamma}^2 \tag{1}$$

where ρ is the material density of the particles, and $f(\xi)$ is a functional form of the structure of the granular materials. For his system, Bagnold proposed $f(\xi) = \lambda^2$ where:

$$\lambda = d/s, \tag{2}$$

is the "linear concentration"; here, s is the mean distance between particles (e.g., Fig. 1 (a)). Bagnold demonstrated that for certain particle arrangements $\lambda = ((\nu_{max}/\nu)^{1/3} - 1)^{-1}$ where ν_{max} the maximum solids fraction, ~ 0.74 for uniform spheres. Others (e.g., Refs. [8], [9]) have shown the general form of Equation 1 applies to a broader range of monosized systems, using different forms for $f(\xi)$ [8] and $f(\xi)d^2$ [9].

These and other realizations of Equation 1 contain dependencies on particle size distribution. For a mixture of different sized particles, it is not obvious what the representative size

should be, nor what one might use for ν_{max}. Further, for the typical disorder that arises in a mixture of different sized particles there is not a clear lengthscale over which two particles should be considered neighbors based on which an average s should be calculated (e.g., Fig. 1(b)).

Recently, significant advances have been made in understanding pressure and structure associated with quasi-static deformation of monosized granular materials above the jamming transition, i.e., systems where the solids fraction ν is greater than the minimal solids fraction required for mechanical stability ν_c [10]-[15]. For example, simulations (e.g., [10]) and experiments [12] have shown $p \sim (\nu - \nu_c)^\beta$ where β depends on the contact interaction potential between particles. Their results further suggest a power law relationship between the number of contacts per particle, Z, and p. These results suggest an alternative approach for continuously sheared mixtures where information regarding how the particle size distribution affects packing may be contained in measures of the structures such as Z.

We probe the dependence of boundary pressure associated with dense sheared granular mixtures on their particle size distributions using simulations of binary mixtures of different sized particles. We find there is a nonmonotonic dependence of p on the average particle size $\overline{d}$. We demonstrate this can be modeled using a relationship between effective packing efficiency and Z through a formulation derived for the packing for monosized systems of spherical particles near the jammed state [14], [15].

For our simulations we use a soft sphere Discrete Element Method (DEM) [16]. Particle-particle and particle-wall contact forces are represented using a non-linear force model according to Hertzian and Mindlin contact theories and some experimental parameterization [17] [18]. For most of the results described here the particles have material properties similar to quartz [18]. We discuss similarities and differences using softer particles near the end.

We primarily simulate binary mixtures of 10 mm and 20 mm particles (with a polydispersity of 10% in the diameter of each component to inhibit crystallization). The particles are sheared in a plane Couette cell (as in Fig. 2) in the absence of gravity similar to Bagnold's experiments [6] and simulations performed by daCruz et al. [8]. Two parallel walls contain the particles in the y-direction, one of which moves with constant velocity U_w as illustrated in Fig. 2(a). The boundaries are periodic in the other two directions. Most of the simulations are constant volume simulations. For these, the Couette cell has dimensions of height $H = 240$ mm, length $L = 288$ mm (in the streamwise direction) and breadth $B = 150$ mm.

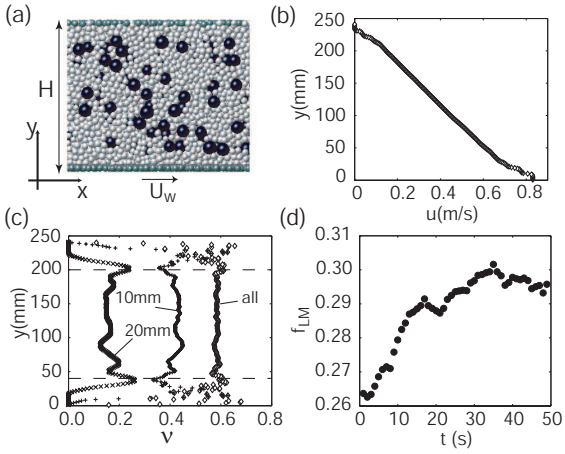

FIG. 2: (a) Image from one time step in a parallel Couette cell simulation described in the text for $f_L = 0.25$. U_W =830mm/s ($\dot{\gamma} = 3.44s^{-1}$) (b)-(d) Some kinematics for the mixture shown in (a). (b) Streamwise velocity profile. (c) Solid volume fraction profiles for each component of the system and the mixture. (d) The fraction of large particles in the central region, i.e., $f_{LM} = \nu_{20mm}/\nu_{mix}$ for the region within the dashed lines shown in (c) ($y = [40, 200]$mm).

The total mass of the particles is $\sim 15.6kg$ for all simulations we report here, resulting in a solids fraction of $\sim 56.8\%$. We also perform constant pressure simulations, which we discuss shortly. To minimize particle slipping at the top and bottom boundaries, we affix 10 mm particles to the walls in a random array [19].

Under these conditions the velocity profile is linear (Fig. 2(b)) and segregation is minimized (Figs. 2(c)-(d)). Initial segregation of large particles away from the walls is minimal and quickly stabilizes, as illustrated by the temporal plot of the fraction of large particles f_L in the middle section shown in Fig. 2(d). There is no segregation in the streamwise direction. Thus, these boundary conditions effectively isolate the effect of particle size distribution on the boundary pressure.

Boundary pressures are obtained by summing the $y-$components of all forces on the particles affixed to the boundary and dividing the sum by LB. The pressure data fluctuate but stabilize after approximately 10s. The probability distribution function of the boundary pressures after steady state is reached is essentially lognormal [20] so we consider the average well-behaved. We report the average pressure p for the second 10 seconds of data from several computational experiments where the shear rate $\dot{\gamma}$ and f_L are varied from one experiment to the next: $\dot{\gamma} = 3.44s^{-1}$ to $11.44s^{-1}$, and f_L=0 to 1. The average particle size for each

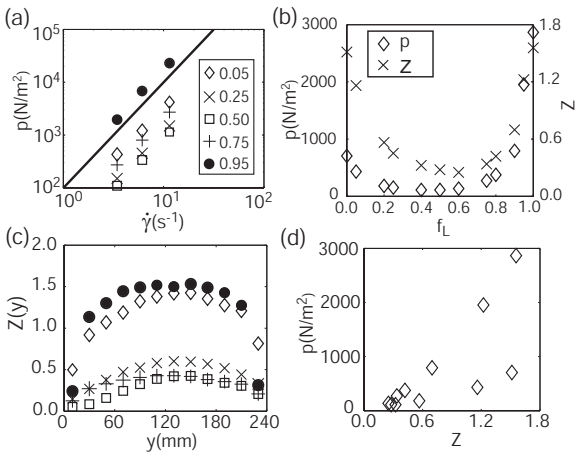

FIG. 3: (a) p vs. $\dot{\gamma}$ for several fractions of large particles as indicated in the legend. The solid line represents a slope of two. (b) p and Z vs. f_L for $\dot{\gamma} = 3.44s^{-1}$. (c) Profile of $Z(y)$ for several fractions of large particles (symbols indicated in (a)). A minor asymmetry persists associated with the initial configuration of the particles. (d) Parametric plot of p as a function of Z for the results shown in (b).

mixture $\overline{d}$ is approximately proportional to f_L: $\overline{d} \sim 10(1 + f_L)$ mm.

Figure 3(a) shows p as a function of $\dot{\gamma}$ for different values of f_L. As in Equation 1, for any particular mixture $p \sim \dot{\gamma}^2$. However, for any particular value of the shear rate, the pressure does not depend monotonically on average particle size. As f_L increases, the normal stress first decreases then increases. This is made particularly clear by plotting p vs. f_L for one particular shear rate ($\dot{\gamma} = 3.44s^{-1}$) in Fig. 3(b). Plotting boundary shear stress τ vs. $\dot{\gamma}$ and vs. f_L yields similar trends. We focus here on developing a model for the variation of p with particle size distribution and comment on the extension to τ and $\mu^* = \tau/p$ in the summary.

We consider results for monosized granular materials near the jammed state suggesting a power law relationship between p and Z [10]-[13]. In our mixtures, $Z(y)$ is sensitive to minor variations in particle concentration and segregation (Fig. 3(c)), so we consider the value averaged across the cell Z and plot it as a function of f_L along with p in Fig. 3(b). Both Z and p follow the same trend as f_L is varied. However, in a parametric plot of p vs. Z [Fig. 3(d)], in contrast with monosized systems near the jammed state [10]-[13], there is no simple relationship between p and Z for steadily sheared mixtures.

We propose that the differences between the dependence of p on Z in monosized systems and in our mixture is related to the variability of the potential packing efficiency from one

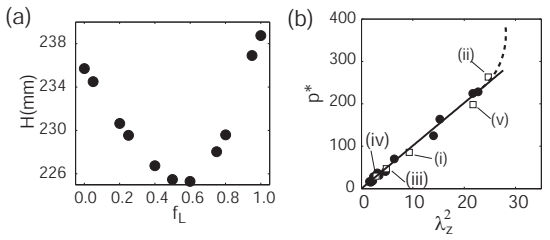

FIG. 4: (a) H vs. f_L for several values of f_L, in constant pressure simulations where $p_{app} = 17.2kPa$, and $U_w = 830mm/s$ ($\dot{\gamma} \sim 3.44mm/s$). (b) p^* vs. λ_Z^2 ($k = 1.2$) for several mixtures, $\nu = 0.568$: those from Fig. 3(b) (•), and those where $\overline{d} = 15$mm: (i)12 & 18mm (ii) 14 & 16mm (iii) 10, 15, & 20mm (iv) 10,12.5,15, 17.5, & 20mm (v) 15mm particles (□). The solid line shows $p^* = K\lambda_Z^2$, K=10.1; k=1.2. Dashed line indicates limiting results from higher values of p and ν.

mixture to the next under otherwise identical conditions. We investigate this hypothesis by considering the variation in ν with f_L under analogous constant pressure simulations. For these, the mixtures are subjected to the same applied pressure at the boundaries p_{app} and the upper boundary is allowed to move in the y-direction. As in the constant volume simulations, steady state conditions are reached after $\sim$ 10s [20]. In Fig. 4(a) we plot the height averaged over the second 10s of each simulation, for several values of f_L. The trend is similar to that of p vs. f_L (Fig. 3(b)): for the same applied pressure, ν is higher for the mixtures for which $f_L \approx 0.5$ compared to the mixtures for which $f_L \approx 0$ or $f_L \approx 1$. This indicates that while the different constant volume simulations have the same porosity, the free space effectively *available* to the particles in the mixtures for which $f_L \approx 0.5$ is greater than those for which $f_L \approx 0$ or $f_L \approx 1$. We hypothesize that the variability of this effective free space gives rise to a variability of what Bagnold referred to as a *dispersive pressure* [6] - the pressure resulting from interparticle collisions.

To quantitatively model the variation of available free space (and ultimately p) with Z, we evoke concepts associated with free volume per particle W from quasi-static mono-sized systems [14]-[15]. By experimentally measuring Voronoi volumes (V_v) and Z associated with each particle (volume V_p) in a static granular system, Aste et al. [14] showed that $W = V_v - V_p$ scales inversely with Z. Analytical results of Song et al. [15] show that $W = 2\sqrt{3}V_p/Z$. For our constant volume simulations, ν is invariant from one experiment to the next, so for the whole system, $W = (1-\nu)HLB/N$ where N is the total number of particles. However, the *available* free space is somewhat less than that; we define $W_{\text{eff}} \equiv (\nu_{max} - \nu)HLB/N$. For a

computationally accessible measure of W_{eff}, we consider the analytical results of Song et al. [15] and propose a similar relationship between W_{eff} and Z:

$$W_{\text{eff}}/V_p = k/Z. \tag{3}$$

where k is an unknown constant, but must satisfy $k < 2\sqrt{3}$ since $W_{\text{eff}} < W$ [21]. To relate the above discussion to p, we return to Bagnold's λ (Equation 2). Since a direct measure of an average s for our mixtures is ambiguous, we define an effective average space between particles s_{eff} according to W_{eff}. As we sketch in Fig. 1(a), we relate W_{eff} to an effective spacing between particles geometrically via spherical shells, and s_{eff} is twice the thickness of these shells:

$$W_{\text{eff}}(z)/V_p = \pi/6 \left[(d + s_{\text{eff}})^3 - d^3\right] /(\pi d^3/6) \tag{4}$$

We note that for these definitions, s_{eff} and W_{eff} are nonzero at random loose packing [21]. Equating the righthand sides of Equations 3 and 4 and solving for $\lambda_Z \equiv d/s_{\text{eff}}$, we find:

$$\lambda_Z = \left[(k/Z + 1)^{1/3} - 1\right]^{-1} \tag{5}$$

With this, we propose a modified version of Bagnold's model for pressure (Equation 1) associated with dense sheared mixtures of different sized particles: $p \sim \rho\lambda_Z^2\overline{d}^2\dot{\gamma}^2$. Combining this with Equation 5 we consider a dimensionless p:

$$p^* = p/(\rho\overline{d}^2\dot{\gamma}^2) = K\left[(k/Z + 1)^{1/3} - 1\right]^{-2} \tag{6}$$

where K is a proportionality constant. We perform a 2-parameter nonlinear least squares fit to find $k = 1.2$ and $K = 10.1$. We then plot p^* vs. λ_Z^2 in Fig. 4(b) for the data from Fig. 3(b) and analogous results from other size distributions detailed in the caption. The collapse of the data suggest that Equations 5 and 6 provide an extension to Bagnold's classic relationship for pressures [6] associated with dense flowing granular mixtures. The results for τ are similar as one might expect from Bagnold's model which by design predicts p and τ. Interestingly, the power law dependence of τ on λ_Z is slightly different, and there is a dependence of $\mu^* = \tau/p$ on f_L that depends on the boundary conditions as we discuss in another paper [22]. Considering analogies with Bagnold's model, one may also consider whether or not λ_Z is directly related to $\overline{d}$ and s averaged over a length scale that captures the local structure, such as a cluster size or a correlation length [9]. Alternatively, λ_Z may

effectively capture such a measure of structure somewhat independent of $\overline{d}$, issues we are currently investigating.

In addition to providing an extension to Bagnold's stress scaling for mixtures, these results provide some links between some established behaviors of monosized granular materials near the jammed state and dense flowing granular mixtures. Given this, it is interesting to consider the level and limits of their applicability to granular mixtures whose particle and mixture properties vary significantly from those we used for these results. For example, preliminary investigations into the dependence of these results on particle hardness show quantitative differences only for somewhat softer particles. Specifically, for particles with an elastic coefficient up to four orders of magnitude smaller than for the results shown here [18], $p \sim \lambda_Z^2 \rho \overline{\mathrm{d}}^2$. Still, over this range Z increases with decreasing hardness (e.g., Ref. [23]) while W_{eff} does not, so k must depend inversely on particle hardness. In contrast, for systems of significantly softer particles, the rheology changes qualitatively, and p is no longer proportional to $\dot{\gamma}^2$ [23]. Nevertheless, for a constant value of $\dot{\gamma}$ we find a similar non-monotonic relationship exists between p, Z, and $\overline{d}$. While a similar framework may apply to these systems, the full effect of varying particle hardness and indeed other particle properties such as material friction coefficient (e.g., Ref. [24]) is not yet clear. Geometric considerations likely further constrain the applicability for binary mixtures with extreme particle size differences when the size of the smaller particles approach the size of the pore spaces among larger particles ($d_S/d_L \lesssim (2/\sqrt{3} - 1)$).

Finally, preliminary results for somewhat higher and lower values of ν and p indicate a limit for the applicability of Equation 6 even for relatively hard particles. For higher values of p and ν, p continues to increase with little increase in Z as indicated by the dashed line in Fig. 4 (d) possibly as the system is approaching a jammed state. For somewhat lower values of ν, the pressure appears less sensitive to Z possibly as the system is approaching a gaseous state, though segregation and other inhomogeneities increase at lower solids fractions making systematic investigation of this more difficult. More work is needed to flush out these transitions and to determine their dependencies on particle property and shear rate. As a result of the work investigating these details, more of the physics of transitions among different phases of granular fluids and solids may become apparent.

We gratefully acknowledge funding for this research provided by the National Center for Earth Surface Dynamics (NCED), a NSF Science and Technology Center funded under

agreement EAR-0120914, and by NSF grant CBET-0932735. We also thank William E. Dietrich, Leslie Hsu, Deveraj van der Meer, Robert Behringer, Michel Louge, and Vaughan Voller for helpful discussions. This work is carried out in part using resources at the University of Minnesota Supercomputing Institute.

[1] R. Iverson. Rev. Geophysics **35**, 245 (1997).

[2] P. Coussot, and M. Meunier. Earth Science Reviews **40** 209 (1996).

[3] T. Takahashi. Debris Flow: Mechanics, Prediction and Countermeasures. Taylor and Francis Group, London, UK (2007).

[4] L. Hsu, W. E. Dietrich, and L. S. Sklar. J. Geophys. Res. **113** F02001 (2008).

[5] Y. Zhong and K. Minemura. Wear **199** 36 (1996).

[6] R. A. Bagnold, Proc. Roy. Soc. Lond. A **225**, 49 (1954).

[7] L. E. Silbert, G. S. Grest, R. Brewster, and A. J. Levine, Phys. Rev. Lett. **99**, 068002 (2007).

[8] F. daCruz, S. Emam, M. Prochnow, J.-N. Roux, and F. Chevoir, Phys. Rev. E **72**, 021309 (2005).

[9] O. Baran, D. Ertas, T. C. Halsey, G. S. Grest, and J. B. Lechman, Phys. Rev. E **74**, 051302 (2006).

[10] C. O'Hern, S. A. Langer, A. J. Liu, and S. R. Nagel, Phys. Rev. Lett. **88**, 075507 (2002).

[11] S. Henkes and B. Chakraborty, Phys. Rev. Lett. **95**, 198002 (2005).

[12] T. Majmudar, M. Sperl, S. Luding, and R. P. Behringer, Phys. Rev. Lett. **98**, 058001 (2007).

[13] J. Zhang, T. S. Majmudar, A. Tordesillas and R. P. Behringer, Gran. Matt. *in press* (2010).

[14] T. Aste, M. Saadatfar, and T. J. Senden, J. Stat. Mech. P07010 (2006).

[15] C. Song, P. Wang, and Hernán A. Makse, Nature **458** 629 (2008)

[16] P. A. Cundall and O. D. L. Strack, Géotechnique **29**, 47 (1979).

[17] Y. Tsuji, T. Tanaka, and T. Ishida, Powder Tech. **71**, 239 (1992).

[18] $F_n = -k_n\delta_n^{3/2} - \eta_n\delta_n^{1/4}v_n$ and $F_t = min\{-k_t\delta_n^{1/2}\delta_t - \eta_t\delta_n^{1/4}v_t, \mu F_n\}$ are forces perpendicular and parallel to the plane of contact; the numerical parameters are derived for typical properties of quartz. Specifically, for d=10mm: $k_t = 1.9 \times 10^9 N/m^{3/2}$, $k_n = 1.4 \times 10^9 N/m^{3/2}$, $\eta_t = 1.1 \times 10^2 Ns/m^{5/4}$, $\eta_n = 9.8 \times 10^1 Ns/m^{5/4}$, and $\mu = 0.5$. For our 50/50 mixtures sheared at $\dot{\gamma} = 3.44s^{-1}$, the average collision time is $10^{-4}s$; the average time between collisions is $10^{-3}s$,

and $\dot{\gamma}^{-1} \sim 0.3s$.

[19] The "glued" particles have the same material properties as the flowing particles. Results appear independent of the size of these particles provided they are large enough to provide sufficient roughness and arranged to prevent small particles from being preferentially trapped.

[20] B. Yohannes and K. M. Hill, in *IUTAM-ISIMM Symposium on Mathematical Modeling and Physical Instances of Granular Flows, 2010*, eds. J. Goddard, J. T. Jenkins, and P. Giovine (Reggio Calabria, Italy, 2009) p. 379.

[21] We note that this model is limited to continuously unjammed sheared system, so that $\nu < \nu_c$, $W_{\rm eff} > 0$, and Z remains bounded. While it cannot be tested without a known form for $nu_{\rm max}$ for mixtures, it suggests a from from which $nu_{\rm max}$ may be predicted.

[22] B. Yohannes and K. M. Hill, under review (2010).

[23] R. Brewster, L. E. Silbert, G. S. Grest, and A. J. Levine, Phy. Rev. E **77**, 061302 (2008).

[24] C. Campbell, J. Fluid. Mech. **465**, 261 (2002).